

WIRELESS, IN-VESSEL NEUTRON MONITOR FOR  
INITIAL CORE-LOADING OF ADVANCED BREEDER REACTORS\*

J. T. De Lorenzo    T. V. Blalock\*\*    M. M. Chiles  
E. J. Kennedy\*\*    J. M. Rochelle    K. H. Valentine

Oak Ridge National Laboratory  
Oak Ridge, Tennessee 37830

### Abstract

An experimental wireless, in-vessel neutron monitor is being developed to measure the reactivity of an advanced breeder reactor as the core is loaded for the first time to preclude an accidental criticality incident. The environment is liquid sodium at a temperature of  $\sim 220^\circ\text{C}$ , with negligible gamma or neutron radiation. With ultrasonic transmission of neutron data, no fundamental limitation has been observed after tests at  $230^\circ\text{C}$  for  $>2000$  h. The neutron sensitivity was  $\sim 1$  count/s-nv, and the potential data transmission rate was  $\sim 10^4$  counts/s.

### I. Introduction.

An experimental in-vessel monitor was designed and fabricated and is being further developed to ultrasonically transmit reactivity data from advanced breeder reactors. Since such reactors have potentially high reactivity cores, their initial fuel-loading operation will require careful surveillance as the core is loaded to preclude an accidental criticality incident.

An in-vessel neutron detector is preferred to an ex-vessel detector because it is closer to the fuel elements and is not shielded by blanket assemblies. Thus, data from an in-vessel detector are received at a greater rate (up to  $10^4$  counts/s for this model) and are more easily interpreted. Also, with an in-vessel detector, the neutron source required to make the sub-criticality measurements can be reduced in size and possibly eliminated.

A wireless, completely remote in-vessel detector can be located at any core position, giving much greater versatility to the measurements. In addition, the wireless detector does not need expensive instrument thimbles and does not inhibit the motion of fuel handling equipment.

The in-vessel environment for this initial start-up monitor is liquid sodium at a temperature of about  $220^\circ\text{C}$ . No existing neutron monitor has the wireless capability and adequate sensitivity for this application. The experimental model described herein has been successfully tested at  $230^\circ\text{C}$  for  $>2000$  h.

### II. Wireless Neutron Monitor Concept

The current concept of the wireless neutron monitor system is shown in Fig. 1. In the sodium-filled reactor vessel (0.6 m diam  $\times$  18 m high), the neutron monitor is positioned in the reactor core region within a dummy fuel element. The ultrasonic transmitter is

\* Research sponsored by the Division of Reactor Research and Technology, U.S. Department of Energy under contract W-7405-eng-26 with the Union Carbide Corporation.

\*\* Department of Electrical Engineering, University of Tennessee, Knoxville.

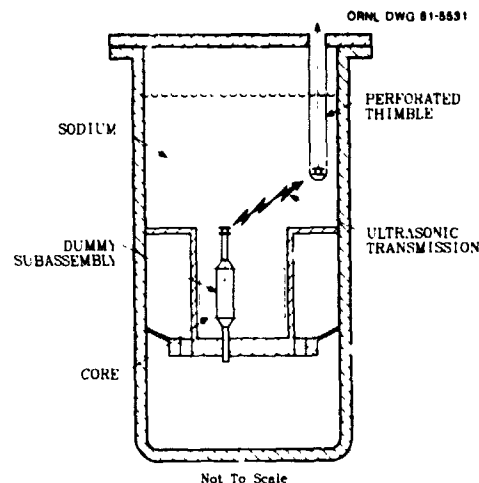


Fig. 1. Concept of a wireless, initial core-loading neutron monitor for an advanced breeder reactor.

mounted at the top end of the dummy element where it can transmit signals along an unobstructed path through the sodium to a receiver which is also immersed in the sodium.

### III. Instrumentation

A diagram of the instrumentation is shown in Fig. 2. A fission counter senses the neutrons, and the resulting electrical pulses are processed by a pulse amplifier and a bandpass filter with single-pole upper and lower cut-off frequencies (RC-CR filter). Electronic noise and alpha pile-up noise are rejected by a discriminator. The discriminator output pulses trigger a driver circuit which excites a 2 Mc ceramic crystal to create an ultrasonic burst for each neutron pulse exceeding the discriminator threshold level. The primary electrical power, which will be derived from a radioisotopic thermoelectric generator, is transformed by a dc-dc converter to positive and negative 10 V levels to bias the fission counter and to drive the active circuitry.

The total quiescent power of the instrumentation at a temperature of  $230^\circ\text{C}$  is 0.56 W with a dc-dc converter efficiency of 0.6. The ultrasonic driver is expected to require 0.1 W at an output pulse rate of  $10^4$  counts/s. The primary source requirement is 8.0 V at 0.6 W.

#### A. Fission Counter

A commercial fission counter (Reuter-Stokes model RSN-10A) with a 4-mm electrode spacing,  $1000\text{-cm}^2$  of sensitive area, and a  $300^\circ\text{C}$  maximum operating temperature was selected for our use. These features were required for our special application, and the availability of the counter eliminated a costly in-house fabrication program. However, some special alterations were needed to ensure adequate performance (voltage

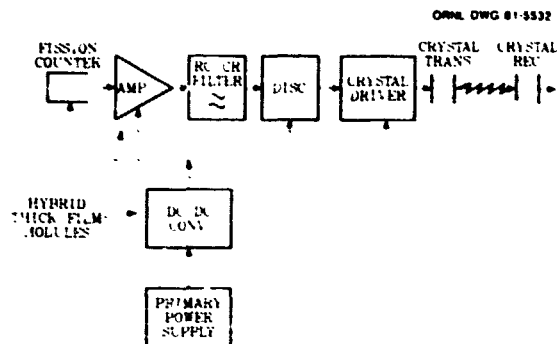


Fig. 2. Block diagram of the instrumentation.

saturation, collection time, and ratio of fission pulse amplitude to alpha pile-up) at a limited counter bias of 10 V. These alterations included an electrode coating of highly enriched  $^{235}\text{U}$  (99.6%) and a gas-filling of Ar-0.01%  $\text{CO}_2$  at  $\sim 10^5$  Pa of absolute pressure.

### B. Amplifier-Filter-Discriminator (AFD)

This module<sup>2</sup> processes signals from a fission counter with an electron collection time near 1.0  $\mu\text{s}$ . The input amplifier is voltage sensitive. To achieve input bias stability at temperature, the input resistor is 20  $\text{k}\Omega$  maximum. This resistor value, coupled with the 150 pF counter capacitance, determines the input integration time constant and a significant fraction of the input noise of the pulse amplifier.

Two other gain stages, each with a voltage gain of  $\sim 16$  per stage, produce output pulses in the range of 1-3 V amplitude. A bandwidth of 5 MHz per stage is more than adequate to amplify the voltage pulse developed at the input.

Capacitive coupling between stages eliminates dc instability problems. One coupling time-constant determines the high-pass frequency of the filter; the low-pass response is controlled by integration in the output stage.

A monostable multivibrator-discriminator generates a logic pulse of 5.6 V amplitude and 5  $\mu\text{s}$  width for each amplifier pulse that exceeds its threshold.

Except for two diodes and a 1-M $\Omega$ , thin-film resistor chip in the discriminator, the entire circuit is fabricated around four, dielectrically isolated, IC, differential operational amplifiers, Harris type HA2625. One of these amplifiers with appropriate positive feedback constitutes the monostable multivibrator-discriminator combination.

### C. Ultrasonic Transmitter

From an analysis of the system,<sup>3</sup> a 2-MHz carrier frequency with pulsed modulation was judged to be most power efficient for the ultrasonic, data transmission process. With an assumption that the receiver bandwidth must be 200 kHz to obtain the maximum data rate,  $\sim 240 \mu\text{W}/\text{m}^2$  of received signal power is required to yield a signal-to-noise power ratio of  $>100$ . This assumes an acoustic noise power density of +10 dB referenced to  $10^{-12} \text{ W}/\text{m}^2\text{-Hz}$ . To create a transmitted beam having a cylindrical wavefront with this intensity at 4 m, nearly 70 mW of pulse power is required to allow for losses in the transmitter drive circuit, the crystal transducer, and the liquid-sodium signal transmission path.

The transducer will contain a PZT-5A ceramic crystal similar to that used by the Hanford Engineering Development Laboratory (HEDL)<sup>4</sup> in their under-sodium viewing systems. It is attached to the transducer face-plate with either a Pb-Sn-Ag solder alloy or a high temperature epoxy. Both have been successfully tested.

The transducer is driven by two VMOS transistors in parallel, with the power being obtained directly from the primary power source. A 2.5- $\mu\text{F}$  Teflon capacitor is currently used as an energy storage element to reduce the ripple on the primary power source.

The crystal impedance is integrated into a resonant tank in the drain circuits of the VMOS transistors. A step-up transformer wound on a high-temperature ferrite toroid reduces the amplitude of the voltage pulses on the drain circuitry.

### D. DC-DC Converter

The dc-dc converter<sup>5</sup> is an astable multivibrator that drives an n-channel VMOS switch (two in parallel) in a dual-coil switching regulator. A dielectrically isolated, IC, differential operational amplifier in conjunction with a 6.9 V zener diode (an emitter-to-base junction of a Dionics DI3424 dielectrically isolated transistor) senses the positive 10 V output variations and adjusts the off-time of the VMOS (on-time is fixed). Integration in the operational amplifier determines the dominant pole of the forward loop. The astable circuits comprise dual, dielectrically isolated, pnp and npn transistors, Intersil I1137 and I1127, respectively.

The coil is a high-permeability, silicon-steel toroid with a Curie temperature of 730°C and is wound with 30 gauge, Teflon-insulated copper wire. The switching frequency is  $\sim 60$  kHz, and 10- $\mu\text{F}$  electrolytic capacitors reduce the ripple to acceptable value for a total load of 12.5 mA for a positive and negative 10 V output.

The internal, drain-substrate, p-n junction diode of n-channel VMOS transistors are used as rectifiers. At 230°C, the forward drop is 0.3 V, with a leakage current of  $<200 \mu\text{A}$ , and a reverse voltage of 60 V.

### E. Primary Power Source

Because of its ruggedness and proved performance in numerous space problems, a radioisotopic generator is being considered for the primary power source. Plutonium as  $^{238}\text{Pu}_2\text{O}_3$  is the heat generator, and silicon-germanium forms the thermocouple junctions. The liquid sodium serves as the "cold leg" of the generator system. For an electrical power output requirement of  $\sim 1.5$  W, a heat source of  $\sim 125 \text{ W}_{\text{th}}$  is considered adequate. Contracts are being prepared for the procurement of this source.

## IV. Hybrid Thick-Film Circuits Fabrication Details

The AFD circuit and the dc-dc converter are fabricated with thick-film technology on 51- by 51-mm (2- by 2-in.) and 32- by 32-mm (1.25- by 1.25-in.), 96% alumina substrates, respectively. Figures 3 and 4 are photographs of these two thick-film circuits. The AFD circuit (Fig. 3) was operated at temperatures near 230°C for nearly 2800 h. The metallization is gold (Du Pont 9910). The thick-film resistors are screened

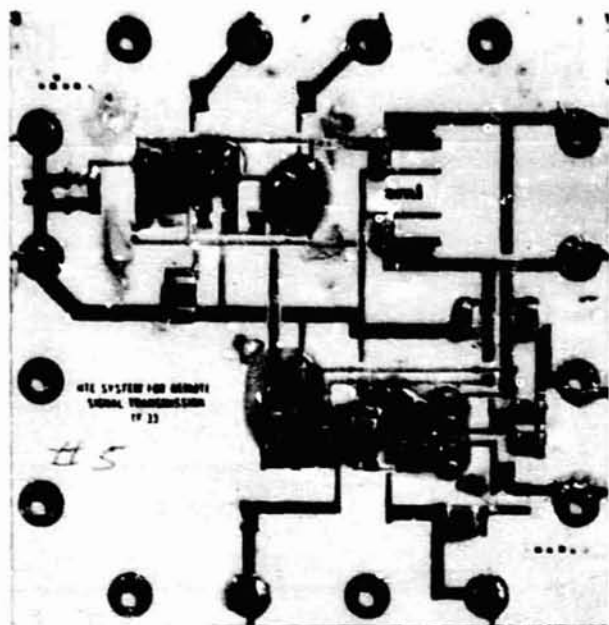


Fig. 3. Photograph of the amplifier-filter-discriminator hybrid thick-film circuit (after 2800 h at  $\sim 230^{\circ}\text{C}$ ).

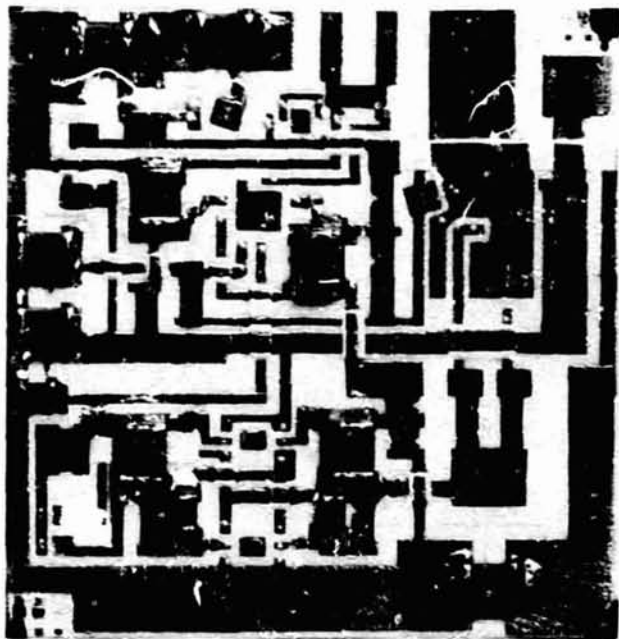


Fig. 4. Photograph of the dc-dc converter hybrid thick-film circuit.

from the Du Pont 1600 Birox series. All semiconductor chips are attached with a silver-filled epoxy (Ablestik 71-1) for electrical attachment to the substrate or with an insulating epoxy (Ablestik 71-2) for isolation. Electrical connections between chip and substrate metallizations are made with 25- $\mu\text{m}$ -diam (1.0 mil) aluminum-0.5% magnesium wire by ultrasonic bonding. All bonds to the gold metallization are mechanically reinforced with an epoxy, either Ablestik 71-1 or Epo-tek P-77. Ceramic covers and a protective semiconductor coating (Dow-Corning R6100) are both used to protect areas of the circuit containing the active elements.

The capacitors contained in these two circuits are monolithic, ceramic capacitor chips with 50- to 100-V ratings. The bypass and decoupling capacitors were formed from a high-dielectric-constant material (X7R), but filter and compensation capacitors were formed from a more stable, low-dielectric material (NPO). A gold-germanium alloy solder ( $360^{\circ}\text{C}$  mp) was used to make electrical connections to the capacitor chips and to the external wires of the substrate using a reflow technique. Later, a parallel-gap welder was obtained to make the external connections with a 25- by 500- $\mu\text{m}$  (0.001- by 0.020-in.) nickel ribbon.

#### V. Description of the Experimental Monitor

The experimental monitor is shown in Fig. 5. Its construction does not represent the construction that would be used in the prototypical monitor. Instead, it was designed to facilitate data taking and to accommodate modifications and improvements as they became apparent during the testing program. From left to right in the figure is the fission counter wrapped in an electrically insulating Teflon jacket to protect the shell of the counter, which is maintained at a negative 10 V biasing potential, followed by the AFD module, the dc-dc converter, and the transformer for the ultrasonic transmitter. At the extreme right is an oil-filled test chamber with a transmitter and receiver crystal at opposite ends. The entire system is mounted on a high-temperature, printed circuit board (Du Pont Pyralin) with a small number of discrete resistors (Addock) and ceramic capacitors (San Fernando Electric). The resistors, capacitors, and the hybrid thick-film modules were attached with 90% lead-10% tin solder. A test pulse, dc and pulse monitor points, oil drain and fill tubes, and thermocouples are all brought out of a flanged end of the assembly. The entire assembly,  $\sim 1.0$  m (40 in.) long, is installed in a cylindrical enclosure, giving a pressure tight containment for an inert cover gas.

#### VI. Test Results and Discussion

The results of the temperature tests of the experimental monitor are summarized in Table 1. The performance of the solid-aluminum electrolytic capacitors was poor, a result not expected based on previous work in high temperature electronics<sup>6,7</sup> and on preliminary tests. Preliminary tests were made in air up to  $275^{\circ}\text{C}$  for hundreds of hours, showing only a slight degradation of performance. The cause of the capacitor failures is believed to be outgassing from oil that leaked out of the ultrasonic test chamber. The oil initially used in the tests possessed inadequate high-temperature properties. Also, the high porosity of the printed circuit board material prevented an adequate clean up of the test assembly.

Two failures of aluminum wire bonds at the gold metallization of the dc-dc converter were the first experienced after nearly 300 successful bonds on other hybrid circuits. This failure rate is not considered excessive at this time, and no changes in our bonding procedures are planned.

Integral bias response obtained for two measurements at  $\sim 230^{\circ}\text{C}$  and covering a time span of nearly 1600 h show only slight differences. Projection of the 1.0 count/s noise curve threshold to the neutron curve shows an  $\sim 75\%$  counting efficiency for the monitor.

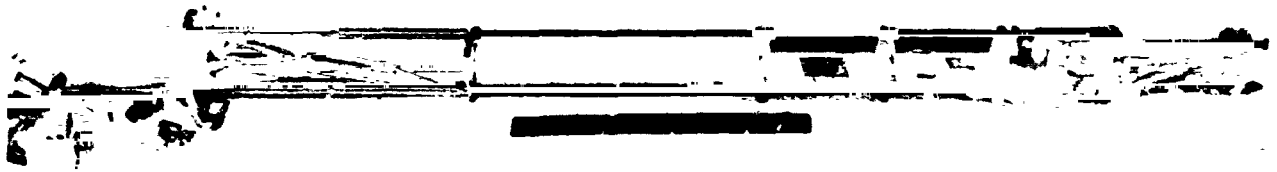


Fig. 5. Photograph of the experimental wireless, initial core-loading neutron monitor (externally powered).

Table 1. Summary of performance of neutron monitor components

Component	Hours at 230°C	Performance
Fission counter	2400	More than adequate
AFB module	2800	Adequate <sup>a</sup>
DC-DC converter	334 <sup>b</sup>	Adequate <sup>c</sup>
Ultrasonic transmitter	2200	More than adequate <sup>d</sup>
Solid-aluminum electrolytics	176 <sup>e</sup>	Not adequate <sup>e</sup>
Printed circuit board, with discrete resistors and ceramic capacitors	2800	More than adequate

<sup>a</sup>Some drift in pulse gain (or amplitude of test signal) not seen in prior 2100-h tests at 250°C.

<sup>b</sup>Maximum time to failure.

<sup>c</sup>Failures caused by two faulty wire bonds at substrate metallization.

<sup>d</sup>Does not include a gated oscillator.

<sup>e</sup>Capacitor failure from outgassing effects.

#### VII. Problem Areas

The failure of the solid-aluminum electrolytics must be resolved. Although the prototypical neutron monitor will not contain an oil source, the apparent sensitivity of these capacitors to outgassing must be determined.

Presently, we are working on a design for a gated, 2-MHz oscillator that will provide the input drive signal for the transmitter. Tests are still to be made on the cylindrical ultrasonic beam generator. The concept for this ultrasonic beam generator is shown in Fig. 6.

#### VIII. Conclusions

Temperature tests on an experimental assembly of an initial-core-loading neutron monitor show no unresolvable problems. Failure of solid-aluminum electrolytics because of off-gassing indicates a need for a vapor-free environment for these devices. Bond failure on the dc-dc converter substantiates the need for pretesting of all hybrid thick-film modules.

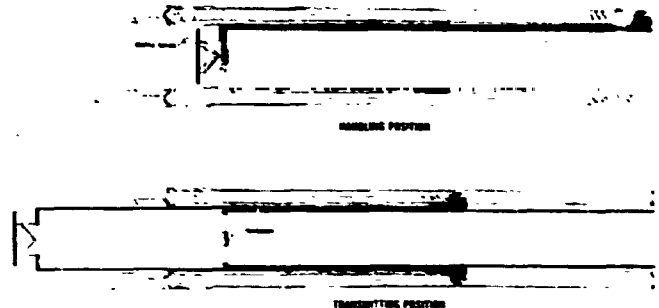


Fig. 6. Conceptual sketch of the cylindrical ultrasonic beam generator.

#### IX. References

1. M. M. Chiles and K. H. Valentine, unpublished work.
2. E. J. Kennedy, T. V. Blalock, J. Phelps, R. Rochelle, and F. Dyer, *Research in Remote Signal Transmission Electronics*, ORNL/Sub-7644/10, Univ. Tenn., Knoxville, Elec. Eng. Dept. (October 1, 1979).
3. J. M. Rochelle, unpublished work.
4. R. W. Smith and C. K. Day, *High Temperature Ultrasonic Transducers for In-Sodium Service*, HEDL-TME 75-21 (January 1975).
5. E. J. Kennedy, T. V. Blalock, S. Genter, P. Mukund, and H. Orrick, *Research in Remote Signal Transmission Electronics, Report II*, ORNL/Sub-7685/7, Univ. Tenn., Knoxville, Elec. Eng. Dept. (October 1, 1980).
6. D. W. Palmer, "Hybrid Microcircuitry for 300°C Operation," presented at the 27th Electronic Components Conf., Arlington, Virginia, May 16-18, 1977.
7. D. W. Palmer and R. C. Heckman, "Extreme Temperature Range Microelectronics," *IEEE Trans. Components, Hybrids and Mfg. Technol.*, CHMT-1(4), (December 1978).

#### Acknowledgments

W. L. Kelly of the Department of Energy (RRT Division) is acknowledged for his interest and encouragement for all phases of the work. C. M. Smith and G. C. Guerrant are also thanked for their assistance in the fabrication and testing of the experimental monitor.